International Journal on Science and Technology (IJSAT)
E-ISSN: 2229-7677 ● Website: www.ijsat.org ● Email: editor@ijsat.org

Synthesis characterization and Antimicrobial Evaluation of Gelatin Coated Poly (ethylene glycol)-Hydroxyapatite Nanocomposites

Neha Sanodiya[1], J. Bajpai A. K. Bajpai[2], S.K. Sonwane[3]

[1]Bose Memorial Research Lab
Department of Chemistry, Govt. Model Science College, Jabalpur, M.P. (India)
[2]Department of chemistry, Govt. A. B. College Baihar, Balaghat
nehasanodiya83@gmail.com

Abstract

Nanotechnology is quick growing field of research having very small dimension particles with multidisciplinary applications in industry, pharmacy, medicine etc. Moreover, the nanomaterials also cover areas such as physics, chemistry, biology, agriculture, material science, including engineering and technology. Nanotechnology has also significantly improved comfort of life due to its multilevel applications in the field of energy production and storage, information technology, medical applications and so on.

This study focuses on the synthesis and characterization of a novel nano composite, integrating poly-ethylene glycol (PEG)-grafted gelatin containing hydroxyapatite moieties. The raw material was first compounded and resulting composite were molded into the petridishes. Using Solvent casting process, it is possible to produce scaffolds with mechanical and structural properties close to naturaltrabecular bone.

The chemical and thermal properties of synthesized composites and bionanocomposites were investigated by spectral technique. It was observed that the pores in the scaffolds are interconnected and their sizes range from 80 to 400µm.

It is known that Hydroxyapatite (HAp) is the most applied calcium phosphate as bone substitutes because of its chemical similarity to the natural calcium phosphate mineral present in biological hard tissues.

Key words: Biopolymer, Gelatin, poly-ethylene-glycol, Hydrxoxyapatite, antimicrobial efficiency.

1. Introduction

Because of its bioactive and osteo-conductive qualities, synthetic hydroxyapatite has been employed extensively for biomedical implant applications and bone regeneration1. Furthermore, hydroxyapatite can promote the development of apatite that resembles bone on the implant's surface.

Because of its brittleness, the hydroxyapatite particle is frequently unstable when mixed with saline or patient blood, which prevents it from being used as a template for bone regeneration. The problem has been solved by adding hydroxyapatite to the polymer matrix, which greatly improves mechanical electricity while increasing osteoconductivity and biodegradability. These conditions can be met by using gelatin (GEL) in aggregate with hydroxyapatite [1-3].

The food, pharmaceutical, and photography industries have all made extensive use of gelatin, one of the most popular natural polymers in tissue engineering research. It is a transparent, tasteless protein with the rheological property of thermo-reversible change between sol and gel [4]. The majority of commercial gelatins are typically derived from pig or cow skin, scale, bones, ligaments, and tendons [5]. Gelatin's abundance, high carbon content, low cost, biodegradability, and nontoxicity are all benefits of using it [6]. The rheological characteristics of gelatin-based hydrogels can be changed by varying factors such as photoinitiator and polymer concentrations, UV light exposure duration, and polymerization intensity and duration [7].

Since Gelatin-hydroxyapatite nano-composites have been created in a variety of forms, including powder, membrane, pastes, cements, microspheres, and scaffolds. In situ precipitation or mechanical mixing was used to create the gelatin-hydroxyapatite nanocomposite [9]. It was discovered that the formation of apatite on the composite scaffolds was improved by nanoscale hydroxyapatite. In order to create gelatin-hydroxyapatite nano composites, nano hydroxyapatite was produced and combined with gelatin in varying proportions. Biomedical applications have made extensive use of this polymer, particularly as scaffolds [10]. To allow enough room for tissue formation and to encourage neovascularization, the scaffolds should ideally have a high porosity, a large specific area, an appropriate pore size, and a strongly interconnected pore structure [11].

Additionally, inorganic crystal nucleation, growth, microstructure, and more broadly the characteristics of such mineral-based materials can be regulated by this porosity [12]. Since natural bone contains nanoscale mineral crystals incorporated in the collagen matrix, the inclusion of nanoscale particles is ideal to create a composite with superior mechanical strength10. The polymer composites are made to specifically address the needs of biomedical applications, such as drug delivery systems and tissue engineering. To create appropriate biopolymer composites, the manufacturing method and filler and polymer matrix composition must be carefully chosen. The development of nano composites, in which nanohydroxyapatite particles are embedded in gelatin biomacromolecule matrices, has been attempted recently [13-15].

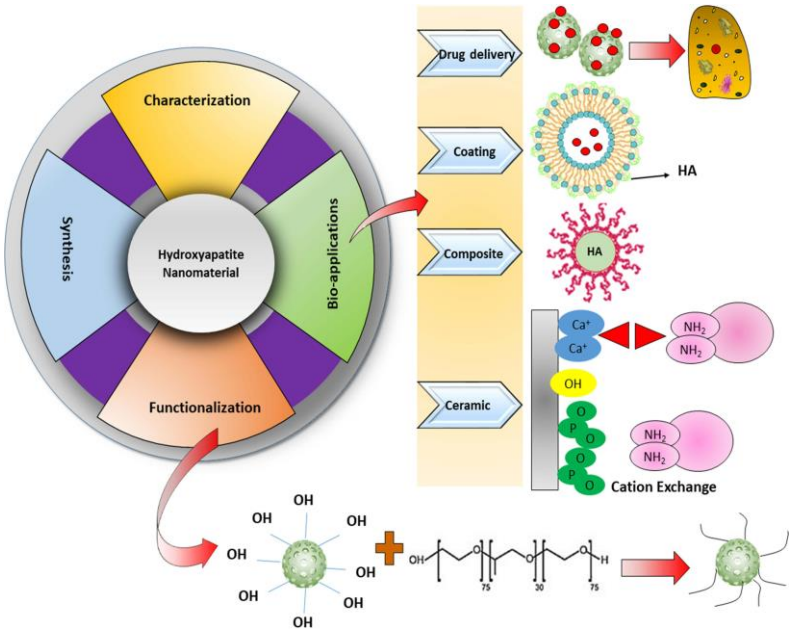

Fig.-1: Graphical Abstract of present study

To address the mechanical issues with bioceramics in bone tissue engineering applications, a great deal of research has been done on both natural (chitosan, collagen, gelatin, silk fibroin) and synthetic (poly-ethylene, polyamide, polystyrene, poly(vinyl alcohol), poly-(ethylene-glycol), and poly-(ether-ketone)) polymers. Gelatin continues to be one of the most popular polymer groups of biomaterials used for medical implants among the aforementioned polymers [16]. This broad range of adaptability is used to customize their applications, including biodegradable scaffolds [17-19], artificial cartilage, and tissue scaffolding [20-21]. Hydroxyapatite nano rod embedded chitosan composites were created in a controlled environment thanks to the excellent combination of the synergistic effect, biocompatible hydroxyapatite, and tunable biodegradability of the polymer matrix [22].Using calcium nitrate $Ca(NO_3)_2.4H_2O$ and diammonium hydrogen phosphate $(NH_4)_2HPO_4$ as starting materials, the current work elaborates on the synthesis of nano-structured hydroxyapatite by chemical method and nano-structured Gelatin coated polyethylene glycol-hydroxyapatite bionano-composite by freeze drying method using calcium hydroxide and ammonium dihydrogen phosphate as starting materials with the help of PEG and gelatin macromolecules. molecular interactions, thermal stability, hydro-philicity, and surface free energy of the prepared nano calcium-hydroxyapatite, PEG-HAp nanocomposites and Gelatin-(PEG-HAp) bio-nano-composites were characterized by Scanning electron microscopy (SEM), X-ray diffraction (XRD), Fourier transform infrared spectroscopy (FTIR), thermo-gravimetric analysis (TGA) techniques etc. The synthesized Gelatin-(HAp-PEG) biononocomposites was tested antibacterial effect against Gram -ve bacteria Escherichia coli. and The composites' cytotoxicity was evaluated using MC3T3-E1 cell line pre-osteoblasts and cultivated L929 cell line fibroblasts.

2. Methods and Materials:

Sigma Aldrich supplied the gelatin powder, polyethylene glycol (MW 6000), $Ca(NO_3)_2.4H_2O$ (99 %), $(NH_4)_2HPO_4$ (99 %), and ammonia. Deionized water of high purity was used throughout the entire experiment. Analytical-grade reagents, calcium nitrate tetra hydrate and di-ammonium hydrogen

phosphate, served as the starting materials for the synthesis of hydroxyapatite nanoparticle. Absolute ethanol and phosphoric acid were of analytical grade, commercially obtained and were used without further modifications.

Synthesis of HAp Nanoparticles

HAp was synthesized by modified wet chemical method. At 25 °C, A solution of 4.06 gm $(NH_4)_2HPO_4$ was dissolved in 100 ml volume of deionized water and, 11.76 g of $Ca(NO_3)_2.4H_2O$ was dissolved in a 100 ml volume of deionized water in a separate container. Then added both the $Ca(NO_3)_2.4H_2O$ solution and $(NH_4)_2HPO_4$ solution over a period of 30 min. The amount of reagents in the solution was calculated to obtain a Ca/P molar ratio value equals 1.67, corresponding to a stoichiometric Ca-HAp nanoparticles [23]. The precipitation of Ca-HAp nanoparticles can be described by the following reactions (1) and/or (2)

$$10\ Ca^{+2} + 6\ H_2\ PO_4^{-} + 2\ OH^{-} \rightarrow Ca_{10}(PO4)_6\ (OH)_2 + 6\ H^{+} \quad (1)$$

$$10\ Ca^{+2} + 6\ H_2\ PO_4^{-} + 2\ OH^{-} \rightarrow Ca_{10}(PO4)_6\ (OH)_2 + 12\ H^{+} \quad (2)$$

After ripening for a specified period (24 h) at room temperature, the precipitates are recovered by centrifuge and then washed with deionized water. Five cycles of washing and centrifuging were repeated to ensure complete removal of the by-product. The calcination of the synthesized powders is performed at 800°C for 1 h in air using a heating rate at 3.0°C/min in an electrical tube furnace from room temperature to 800°C after drying the sample in freeze-drier for 10 h.

The pH of the slurry was measured digitally during the precipitation reaction, reaching a final value of pH 10.5. After ripening for a specified period (24 h) at room temperature, the precipitates are recovered by centrifuge and then washed with deionized water. Five cycles of washing and centrifuging were repeated to ensure complete removal of the by-product. After drying the product in a freeze-drier for 12 hours, the synthesized nanoparicles are calcined at 800°C for one hour in air using a heating rate of 3.0°C/min in an electrical tube furnace.

Synthesis of the Gela-HAp composites

The first step is to solubilize 2.3 g of monobasic ammonium phosphate $[(NH_4).H_2PO_4]$ in 75 mL of deionized water at 45 °C. Afterward, 3.75g (5% w/v) of gelatin powder was added to the solution under stirring for 1 h and a half at a temperature of 45 °C. The pH of the solution was then adjusted to 10 using ammonium hydroxide (NH_4OH) 25% v/v. The second solution was prepared using 7.85g of calcium nitrate tetrahydrate [Ca(NO3)2].4H2O in 60 mL of deionized water at 45 °C. Afterward, 3.0g (5% w/v) of gelatin powder was added to the solution under stirring for 1 h and a half at a temperature of 45 °C. The Ca and P precursors were dissolved in distilled water separately, at the mole fraction ratio [Ca]/[P] = 1.67. Then, carefully by the drip method, 1 drop every 2 s, the first solution (ammonium phosphate) was poured over the second solution (calcium nitrate). This process was done by maintaining vigorous stirring and temperature at 45 °C for 24 h. At the end of the previous stage, the HAP-GEl was frozen in the refrigerator at −20 °C for storage [24].

Preparation of theGelatin Coated (HAp-PEG) Bionanocomposite

The stored HAp−Gel solution was taken for 24 h at a temperature below −20 °C and was lyophilized for 72 h. The composite-to-solvent ratio was set at 1% (w/v) and 5% (w/v) from preliminary tests to maintain the structures of the pores. The amount of cross linking agent Glutaraldehyde (GTA) was set at 2 % (w/v) 0.2 ml , and the amount of PEG varied from 25 % (w/v), 50%, 75% (w/v) to the solvent, for which a solvent based on acetic acid and water (4:1 vol) was used at a temperature of 4 °C for 24 h. At the end of the cross-linking time, the samples were completely submerged in 96% ethanol for 1 h, followed by 70% ethanol for 30 min, and rinsed with distilled water three times to remove chemical residues and neutralize the pH of the composites. At the end of the wash, the samples were again frozen at a temperature below −20 °C for 24 h and lyophilized for 48 h obtaining cross-linked porous composites for the characterization and biological acivity. The identification of the bionanocomposites is summarized in **Table-1.**

Table 1. Composition of the Nanocomposites

Sample	Identification	Composition
Hap-Gel	**NS**	HA and noncross-linked gelatin
HAp-Gel (GTA)	**NS-1**	HA-Gel and GTA (2 % 0.2 ml)
Gel-(Hap-PEG) Bionanocomposites	**NS-1a**	HAp-Gel PEG (25 %)
	NS-1b	HAp-Gel and PEG (50 %)
	NS-1c	HAp-Gel and PEG (75%)

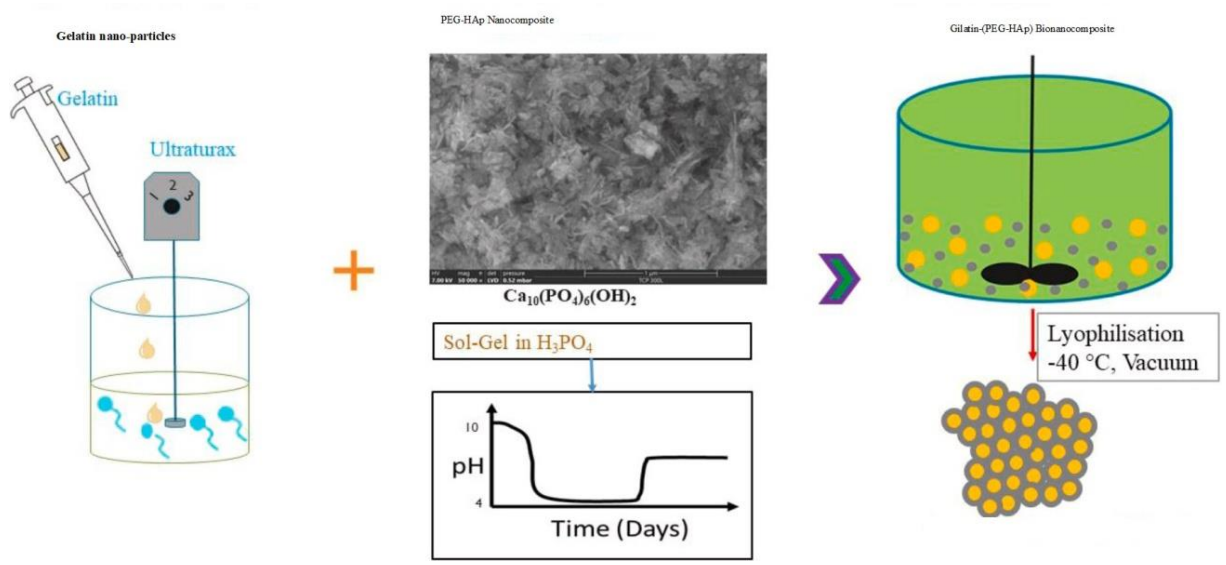

Fig. 2 Schematic illustration of the major steps in the fabrication of the bionanocomposite

Characterization

Using a SN 340, BRUKER OPTIK GmbH, GERMANY instrument, **FTIR (Fourier Transform Infrared Spectrophotometer)** spectroscopy was used to examine the prepared samples. Pellets containing 1 mg of sample and 200 mg of spectroscopic grade KBr were used to obtain the FTIR

spectra in the 450-4,000 cm^{-1} range. Spectra were recorded at 4 cm^{-1} resolution averaging 80 scans. The structure of the samples were analyzed by a **POWDER XRD (Powder X-Ray Diffractometer) ,** D-8 Advance 206890, BRUKER AXS GmbH, GERMANY with CuKa1 radiation (l = 1.5418 Å). The diffraction peak at 25.9º was chosen for calculation of the crystallite size by Scherrer's formula since it is sharper and isolated from others. This peak, which belongs to Miller's plane family (002), depicts the growth of hydroxyapatite crystals along the crystalline structure's axis. FESEM was used to examine the materials' morphology with a **SEM (Scanning Electron Microscope)** NOVA NANO SEM 450, FEI CO. OF USA (S.E.A.) PTE LTD., SINGAPORE, scanning electron microscope and **TEM (Transmission Electron Microscope),** Tecnai G2 30 S-TWIN, FEI CO. OF USA (S.E.A.) PTE LTD., SINGAPORE. Thermal stability and purity of NPs and Composites were investigated using **STA (Simultaneous Thermal Analyzer),** 206.019.242, NETZSCH GERATEBAU GmbH, GERMANY**, HP-TLC (High Performance Thin-Layer Chromatography),** SN1906 W021, CAMAG,SWITZERLAND.

IR Spectrum analysis

Fig. 3 depicts the IR spectra of HAp, PEG-HAP and Gelatin-(PEG-HAp) in order to illustrate the intermolecular interaction between components in the nanoparticles, nano-composite and bio-nano-composite. These spectra exhibited the functional group presence of HAp, HAp-PEG and Gelatin-(HAp-PEG) have performed to characterize the chemical structure of nanoparticles, nanocomposite Bio nanocomposite particles. The materialization of apatite nanocomposites on the substrates is in the form of broad FT-IR bands centered at 569, 603, 963, 1045 and 1091$cm^{-1.}$ These peaks correspond to the first symmetric P–O band and the fourth symmetric P–O band has identified the stretching vibration of the PO_4^{-3}. The fourth phosphate bond is connected to the well-defined and sharp peaks at 569 and 603 cm^{-1}. In addition, the third phosphate band has well defined peaks at 963 and 1045 cm^{-1}.While the sharp peaks at 633 and 3470 cm^{-1} have appeared due to the structural –OH of the apatite. The stretching of the Carbon-oxygen (C-O) bonds in the PEG is responsible for the peak between 1084 and 1748 cm^{-1}.

These peaks seemed due to the polymer that was effectively combined with a large amount of Ca^{2+} through the strong electrostatic attraction presence of negatively charged CH_2–O^- group of PEG to form a covalent bond. the absorption peaks appearing near the wavenumbers of 2924 and 2856 cm^{-1} correspond to the characteristic absorption peaks of methylene and methyl groups respectively, indicating the presence of gelatin biopolymer molecules in Gelatin-(PEG-HAp) bio-nano-compositesIn the spectra, the absorption peaks appearing at 1680~1630 cm-1, 1570~1510 cm^{-1} and 1240 cm^{-1} correspond to the characteristic absorption peaks of the amide I (vC=O), II (δNH+vCN) and III (δNH) bonds of gelatin. Two of them are represented by the amide II bond's characteristic absorption peak. The first is NH, which refers to the N-H bond's bending vibration, and the second is CN, which refers to the C-N bond's stretching vibration. These two vibration absorption peaks are very close and integrated into one peak at 1570~1510 cm^{-1}, so they are collectively called the characteristic absorption peak of the amide II bond. In the Gelatin-(HAp-PEG) spectrum, the absorption peak can be seen at 1643 cm^{-1}.

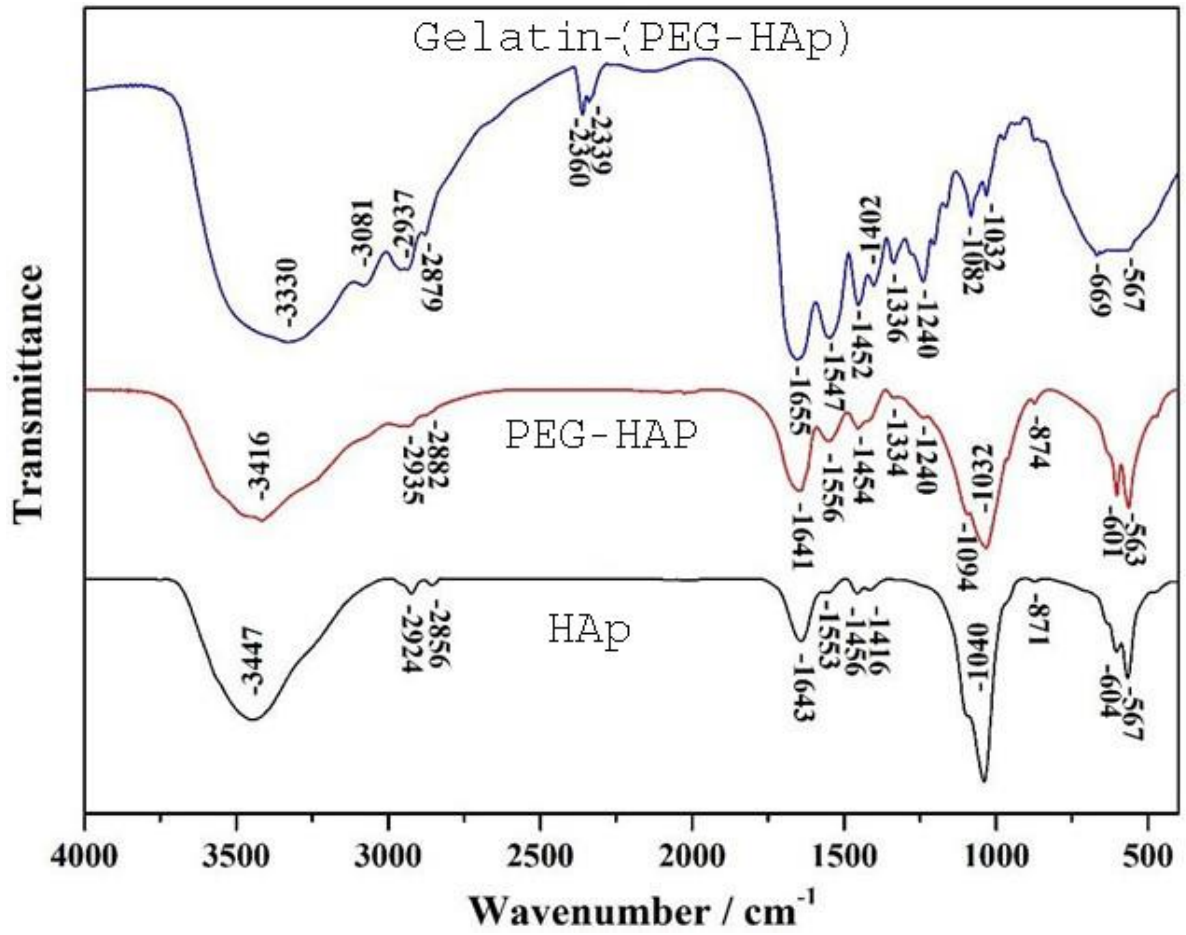

Fig. 3. FT-IR spectra of HAp, PEG-HAp and Gelatin-(PEG-HAp)

XRD Analysis

The XRD patterns of the HAp, PEG-HAp composites and Gelatin-PEG-HAp Bionanocomposite shown in Fig. **4a and 4b**. The diffractogram was recorded from 10 to 80° in 2θ. The step size was 0.0670° in 2θ and the continuous scan step time was 200.02 s. The data was processed using High Score Plus software for background subtraction, peak search, and peak fitting. Monshi-Scherrer's equation **Eq. 1** was used to estimate the crystallite size and peak broadening from the XRD spectral data.

$$\ln\beta = 1/(\cos\theta)+k\,\lambda D \qquad (1)$$

β is full width at half maximum in rad,

θ is peak position (rad),

D is crystallite size (nm), k is Scherrer constant (0.9) and λ the wavelength of the X-ray source (0.1543 nm)

The HAp XRD pattern has distinctive peaks that demonstrate their hexagonal crystalline structure. Other significant peaks are observed at approximately 26 raised to the composed with 26 (002), while a common and intense peak is located around 31.8 raised to the composed with 31.8(2), which corresponds to the (211) plane. The breadth and intensity of these peaks provide information on the

crystallinity, crystallite size, and lattice defects of the nanoparticles. Peaks that are typical of hydroxyapatite (HAp) can be seen in the PEG-HAp nanoparticles' XRD pattern, such as those around 26.5 raised to the composed with 26.5, 31.9 raised to the composed with 31.9, and 32.8 raised to the composed with 32.8. The PEG component typically appears as a broad, amorphous halo, and the intensity and sharpness of the HAp peaks are influenced by the HAp crystallite size and the amount of PEG present. The XRD pattern of gelatin-PEG-HAp bionanoparticles typically consists of peaks typical of crystalline hydroxyapatite (HAp) and features related to the largely amorphous polymeric matrix of gelatin and PEG that are broader and less intense.

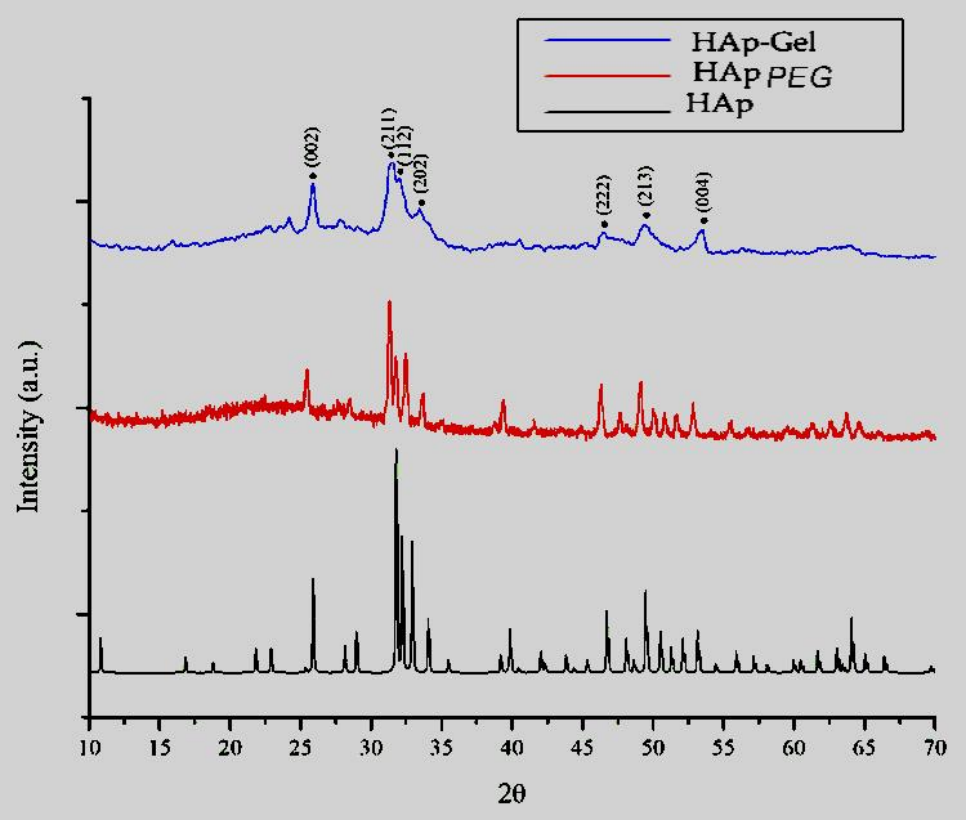

Fig.4a – XRD spectra of HAP/ HAP-Gel/HAp-PEG

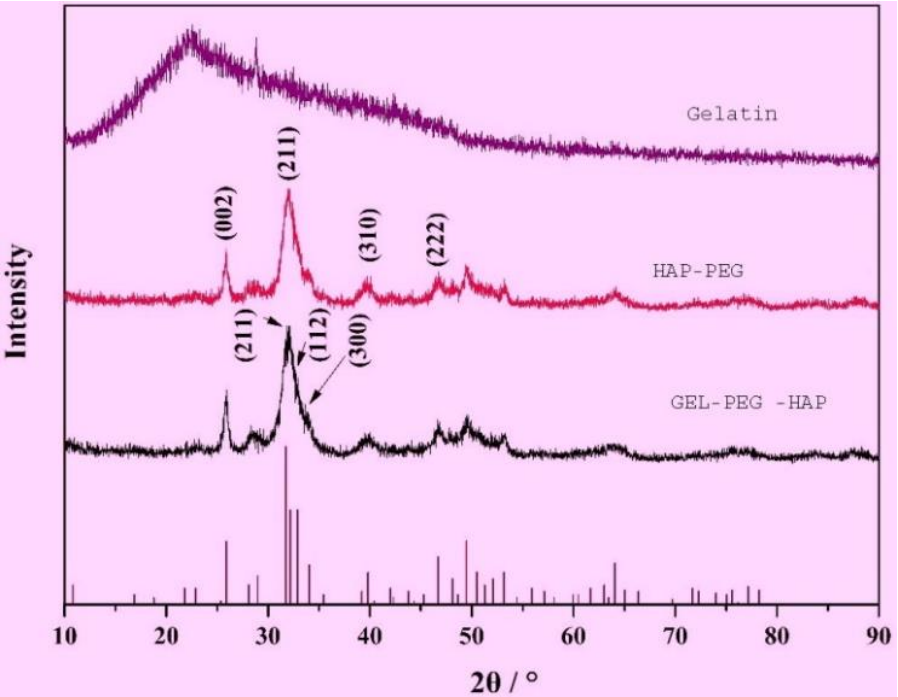

Fig.4b: XRD Spectra of Gelatin /(PEG-HAp)/ Gelatin–(PEG-HAp) bionanocomposite

SEM Image Analysis

The external morphology of nanocomposite particles was studied by scanning electron microscopy (SEM). The formation of amorphous, poor-crystalline, and crystalline bionanocomposite particles of pure HAp, HAp-PEG, and Gelatin-(HAp-PEG) bionanocomposite particles was depicted in SEM images at various magnifications in **Fig. 5.** SEM observations **in Fig. 5 (a, a1)** demonstrate the amorphous powder of pure HAp, and **Fig. 5 (b, b1)** demonstrates the incorporation of HAp particles into the polymer matrix. Additionally, typical images of HAp-PEG demonstrate improved particle behavior in comparison to HAp (pure). The interface between the inorganic and organic phases was indistinguishable due to the high affinity of inorganic crystals for the PEG polymer matrix. Usually HAp particles have been dispersed in respectable solvents for less aggregation and convenient use of biomedical applications. Akhilesh et al., has reported that the PEG polymer can inhibit the agglomeration of inorganic nanomaterials. PEG molecules surrounded the metal ion Ca^{2+} in this instance to form small, dispersed particles because the oxygen group in PEG was responsible for the lower aggregation level in HAp-PEG [38]. The coated Gelatin component has an effect on the surface morphology, as depicted in **Fig. 5 (c, c1)** of Gelatin-(HAp-PEG) nanocomposites. The morphology identifications indicated that the room temperature sol gel method could produce nanoparticles with a good crystal structure. Non-agglomerated nanocomposite particles are visible in the Gelatin-(HAp-PEG) nanocomposites. The delivery of nutrients to the site of tissue regeneration and cell adhesion has both been made possible by these nanocomposite particles.

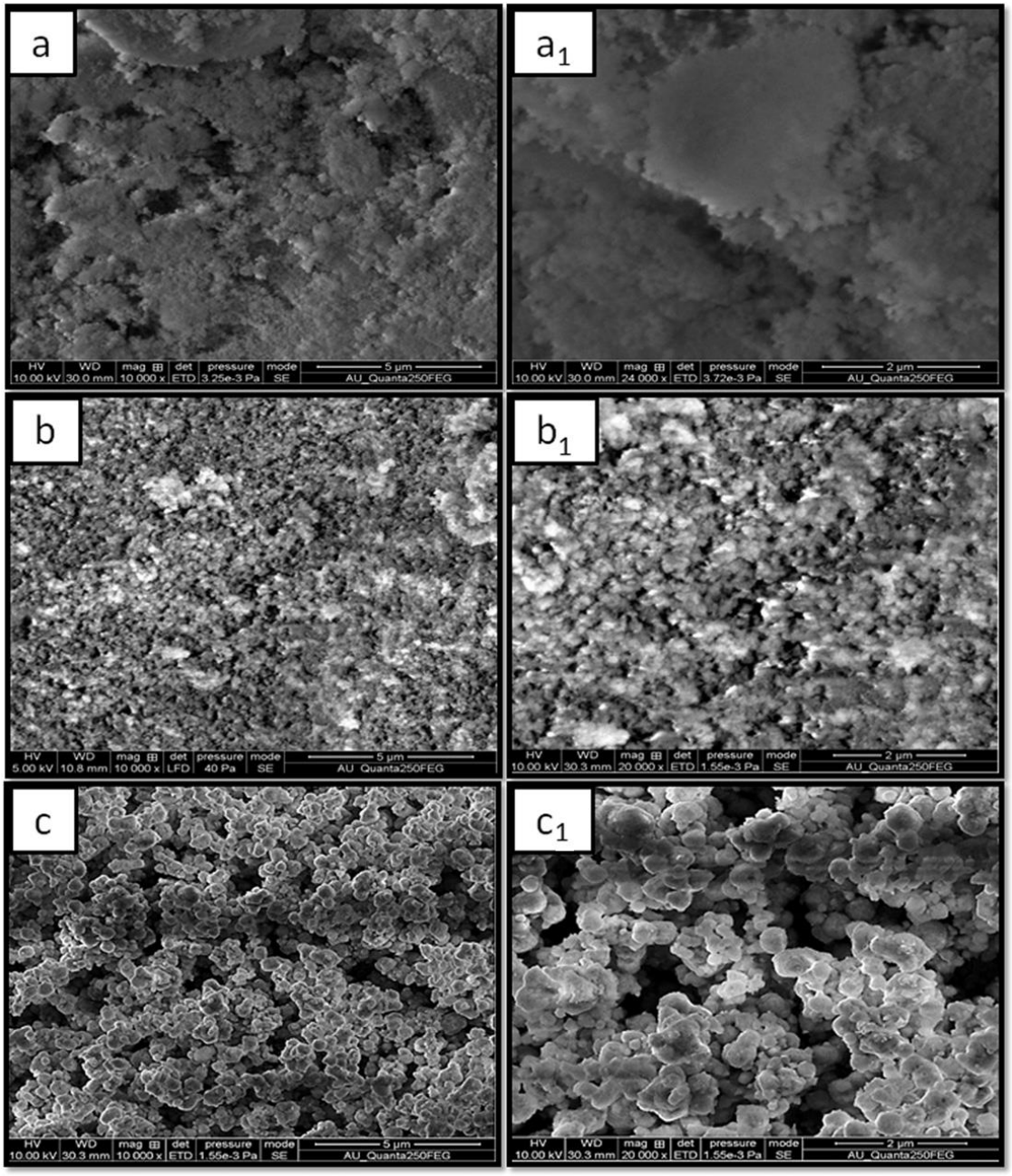

Fig. 5. HR-SEM images of HAp, HAp-PEG and Gelatin (HAp-PEG) in different magnifications.

Swelling Test.

To investigate the swelling capacity of the bionano-composites, the swelling test was conducted following the methodology outlined in the literature [25-26]. Samples from each scaffold group were weighed in triplicate and immersed in PBS (pH 7.5) at 37 °C for the swelling test. Measurements were recorded at the experimental time points of 30 min, 1 h, 3 h, 5 h, 7 h, 10 h, 24 h, 48 h, and 72 h. At each time point, the scaffolds were taken out of the PBS, placed on filter paper for 1 second to eliminate excess surface liquid, and subsequently weighed. The swelling ratio was determined using **equation 2** and was presented as mean ± SD (n = 3) (standard deviation).

$$\% \text{ Swelling} = \frac{Wt - Wi}{Wi} \times 100 \qquad \text{equation 2}$$

Wi = Mass of each lyophilized composite before submerging it into the PBS solution.
Wt = Mass of each composite after the removal of PBS.

The swelling capacities of the composites are illustrated in Figure. The swelling behavior represents a critical parameter for assessing biomedical applicability. An increased swelling rate generally leads to an expanded surface area, facilitating the diffusion of bioactive compounds and the migration of cells into the composite's three-dimensional structure.30,31 The swelling capacity of the composites is depicted in **figure 6**.

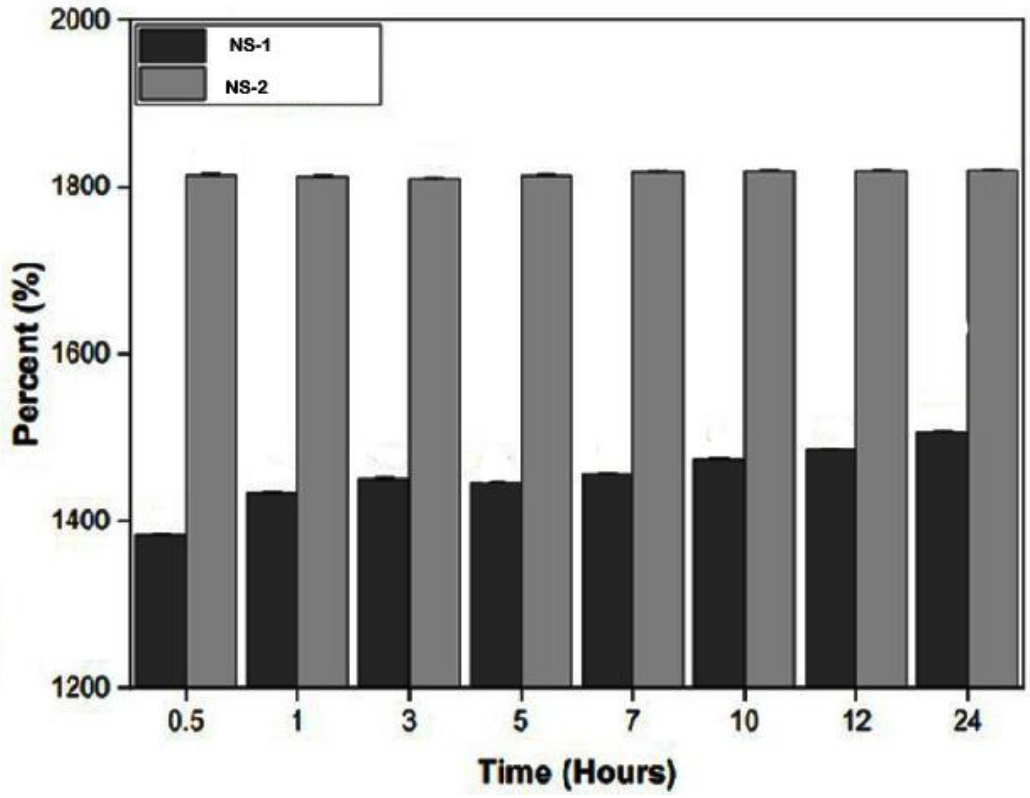

Fig-6: Swelling Test of Bionanocomposites

Composite NS-1 exhibited the lowest swelling rate throughout all experimental durations. Each freeze-dried composite was measured at 20 mg prior to immersion in PBS. Over the time span of 0.5 to 24 hours, composite NS-1 demonstrated a 123% increase in swelling, whereas NS 2, during the same time frame, only increased by 5%. This increase is relatively modest; moreover, in the case of NS 1, it achieved 90% of its swelling capacity within the first 30 minutes of contact with PBS, while NS 2 nearly reached 100%. Initially, a linear relationship between the swelling proportion and immersion time was anticipated until equilibrium was attained, suggesting that equilibrium was achieved within the first 30 minutes of the composites' immersion in PBS. Additionally, after 24 hours, NS 1 and NS 2 recorded swelling rates of 1817.16% and 1506.11%, respectively, resulting in a difference of 313.05% between the two. The degree of crosslinking in each composite significantly influenced the swelling balance of

the composites, revealing that the swelling ratio of HAp and gelatin composites diminished as the degree of cross-linking increased. This finding aligns with existing literature [27-28].

Biological Activity

Agar well diffusion method

The antibacterial activity of the synthesized Gelatin-(HAp-PEG) Bio-nano-composites was screened against Escherichia coli (–ve) using agar well diffusion method with some modifications [29]. In brief, the bacterial cell suspension of 1×10^6 colony forming unit (cfu) mL^{-1} was inoculated using sterile cotton swabs on the Mueller Hinton Agar (MHA) plates. Experimental wells of 6 mm in diameter on the plates were loaded with 20 µg mL^{-1} concentrations of test materials and incubated for 24 h at 37 °C. The experiment included a positive control (Ampicillin alone) and a negative control (Milli Q water without nanocomposite). All the experiments were carried out in triplicate. The zone of inhibition was measured using Antibiotic Zonescale (HiMedia, India). Reduction in bacterial viability was measuring total viable counts at different time in- tervals (0, 6 and 12 h) and bacterial cell death visualized by epi-Fluores- cence microscopy. Fluorescein isothiocyanide (FITC) and propidium iodide (PI) dual stains were used for living and dead cells on bacterium. Propidium iodide penetrates only to damaged cells and binds to the DNA emitting a red color, whereas FITC remains exterior to undamaged cell walls giving rise to green emission [30].

Bacteriostatic (MIC) and bactericidal concentration (MBC)

The MIC and MBC of the Gelatin-(HAp-PEG) Bio-nano-composite were determined according to the method of Ruparelia et al. Fourty microlitres (~ 1×10^6 cells mL^{-1}) of E. coli (–ve) bacterial strain was added to 4 mL of Luria Bertani (LB) broth. The different concentrations (10 to 50 µg mL^{-1}) of the Gelatin-(HAp-PEG) Bio-nano-composite solution was added to the test tubes containing the test bacterial strain. After 24 h of incubation, the MIC results were noted by checking the turbidity of the bacterial growth and the MBC were determined by streaking a loop full of the bacterial culture on the MHA plates, incubated at 37 °C for 24 h. The MBC is the concentration at which the bacteria are completely killed.

Analysis of growth curve

Bacterial colony counting is a convincing technique for the analysis of antibacterial activity of nanomaterials. Antibacterial activity of the synthesized Gelatin-(HAp-PEG) Bio-nano-composite was tested by a standard microdilution method leading to the inhibition of the bacterial growth. E. coli bacterial strain was allowed to grow in 10 mL of LB broth. This media was supplemented with nanocomposite ranging from 10 to 5 µg mL^{-1} and the bacterial cultures were incubated at 37 °C. The growth of test bacterial strains in broth was indexed by measuring the optical density (OD) at 595 nm at regular time intervals using UV–vis spectrophotometer (UV-1800, Shimadzu). The growth curve was plotted between OD595 nm and time [31].

Antibacterial activity of Gelatin-(HAp-PEG) Bio-nano-composite

The consumption of bioceramic polymeric nanocomposite has opened new treatment

avenues in the advanced nanobiotechnological research. In the present investigation, prepared Gelatin-(HAp-PEG) bio-nano-composite exhibited a broad spectrum of antibacterial activity against the test bacterial pathogen. The Gelatin-(HAp-PEG) Bio-nano-composite is thus proved to reduce the bacterial densities significantly even at the least concentration. The results of the composite have given excellent antibacterial activity showed by epifluorescence microscopic images during different time intervals to increase cell death evidenced by mostly the yellow and red staining and very little green was present in it (Fig. 8). However, the broth dilution method inferred the MIC (10 μg mL^{-1}) and MBC (20 μg mL^{-1}) of bionanocomposite against E. coli (Table-4), whereas the bacteriostatic and bactericidal concentrations of antibiotic drug were recorded at 5 and 15 μg mL^{-1} respectively. Stud- ies by some of the researchers have established the nanomaterial im- pregnated nanocomposite as an effective bactericidal material against the various microorganisms [32]. However, there is little information available for the nanocomposite alone in the biomedical applications. In our study we established that the nanocomposite alone has been proved effective antibacterial agents against the test bacterial pathogen. Optical densities were measured and plotted as a function of time at regular intervals between 0 and 24 h with various concentrations (0–50 μg mL^{-1}) nanocomposite (Fig.- 7). Dose-dependent growth dynamics of test bacterial pathogenic strain can be used to assess the relative rate and extent of bactericidal activity of nanomaterials [33]. The growth visibilities of the bacterial strain are treated with various concentrations of the Gelatin-(HAp-PEG) bio-nano-composite. The results showed that the introduction of Gelatin impregnated nanocomposite affected the growth dynamics effectively as compared to the control. Growth of the bacteria was effectively reduced with an increased concentration of nanocomposite, in particular 30 and 40 μg mL^{-1} concentrations of the Gelatin-(HAp-PEG) bio-nano-composite act as effective bactericides and there was an abrupt reduction of bacterial growth [34]. The nanocomposite depicted efficient bacteriostatic and bactericidal properties due to their better efficiency with microorganisms. Earlier researchers have already proved that the different combinations of nanocomposite show an effective antibacterial property against E. coli [35]. The exact inhibitory mechanism of Ca^{2+} nanomaterial and nano-composite on microorganisms is still unknown, the possible mechanism involves the disruption of cell wall of the bacteria which causes structural damages and destabilizes the respiratory chain dehydrogenase and finally causes cell death [36]. The present study supports that the nanocomposite was found to be the potent source of antibacterial biocides against pathogenic bacte- ria. In the future, the necessary efforts will elucidate the antibacterial ef- fect of nanocomposite impregnated HAp and the bacterial contact may improve the antibacterial mechanism by damaging the bacterial cell wall and entering of bionanocomposite or nanoparticles to the cells to kill the bacteria and further it can be developed as an antibacterial agent in biomedical research. These results confirmed that the Gelatin-(HAp-PEG) bio-nano-composite has given good delivery of Ca^{2+} ions on the bacterial surface to reduce the survival of bacteria [37].

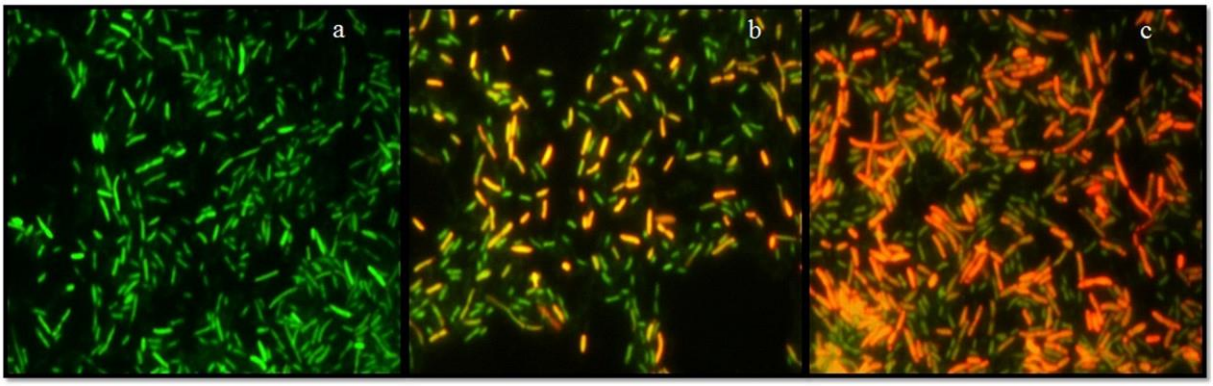

Fig. 7. Epifluorescent microscopic images of bacterial species E. coli
(a) initial, (b) 6 h and (c) 12 h during interfacial contact studies in the presence of HAp-PEG-Ag nanocomposite.

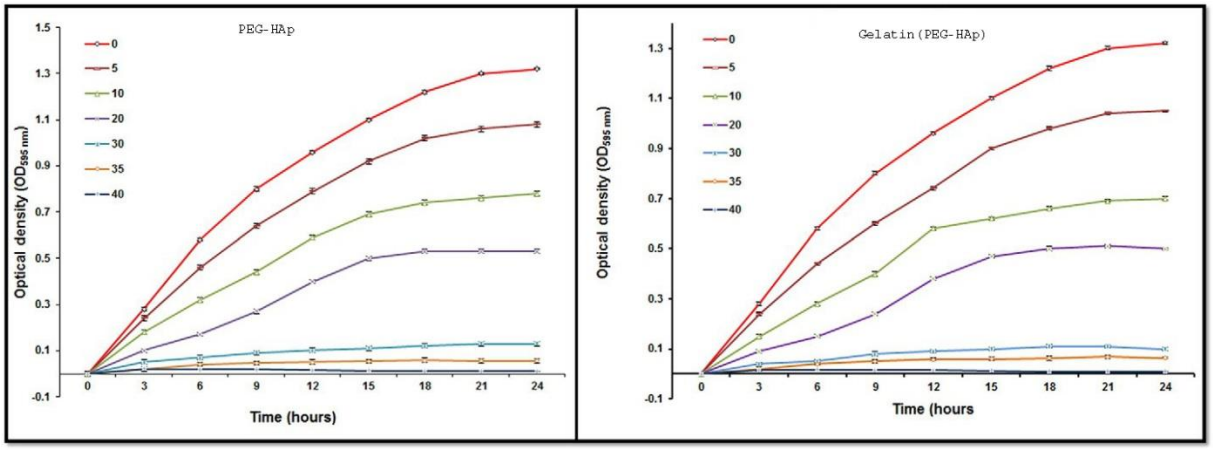

Fig. 8. Effects of the different concentrations of HAp-PEG nanocomposite and Gelatin-(HAp-PEG) against E. coli growth kinetics.

Table 2: Antibacterial activity of Bionanocomposites

Bacterial pathogens	Concentration of nanocomposite (µg Ml^{-1})				Zone inhibition (mm)	
	Gelatin-(HAP-PEG)		HAp-PEG		Gelatin-(HAP-PEG)	HAp-PEG
	MIC	MBC	MIC	MBC		
E. Coli	10	20	10	25	14.6 ± 0.54	13.5 ± 0.5

Cytotoxicity of Bionanocomposites

Cell Culture

The mouse fibroblasts L929 cell line (ATCC CCL-1) and the pre-osteoblasts MC3T3-E1 cell line (ATCC, CRL-2593) were used to investigate the biocompatibility and cytotoxicity of the produced bio-nano-composites. Dulbecco's modified Eagle's medium (DMEM) high glucose (4500 mgL−1), 10% fetal bovine serum (FBS), 1% antibiotic/antimycotic (penicillin 10,000 units.m−1/streptomycin 10

mg.m−1), 1% L-glutamine, and 1% nonessential amino acids were used to cultivate them. Each cell was maintained in a humidified incubator with 5% CO_2 at 37.5 °C [39-39].

Composites Cytotoxicity

To create an eluate for each group, each sample group was weighed at 10 mg, immersed in 1 mL of non-supplemented cellular growth media, and incubated for 24, 48 and 72 hours at 37°C in an environment with a regulated level of 5% CO_2. Following each interval, 300 µL of the original eluate and 300 µL of the medium were used to dilute each eluate at a ratio of 1:1, yielding a second eluate of 5 mg/mL. The plate was incubated for 24 hours after 100 µL of each eluate was added in quintuplicate. Following the incubation period, the plates were rinsed twice with sterile PBS solution. The medium was then changed to DMEM low glucose without phenol red, supplemented with 10 µL of 3-[4,5-dimethylthiazol-2-yl]-2,5-diphenyltetrazolium bromide (MTT) reagent dissolved in PBS at a concentration of 5 mg/mL [40].

Because MTT is photosensitive, the plates were shielded from light. In order to prevent the production of blue crystals, 50 µL of sodium dodecyl sulfate (SDS) detergent solution was added after 4 hours of incubation at 37 °C and 5% CO2. After 15 minutes of shaking, measurements were made using a UV-vis at a wavelength of 570 nm. Equation 1 was used to compute cytotoxicity, with untreated cells serving as the control group [41]. An MTT colorimetric test, which measures the activity of the mitochondrial reductase enzyme in living cells to assess cell viability, was used for the cytotoxicity experiment. The cells were transferred to 96-well plates with a concentration of approximately 6×103 cells/well after being rinsed with PBS and trypsinized with 0.25% trypsin/ethylenediamine-tetraacetic acid (EDTA) for 4 minutes [42].

Each plate was then incubated for 24 hours at 37 °C and 5% CO2. The test involved weighing 10 mg of the sample, immersing it in 1 mL of nonsupplemented cell culture media, and incubating it for 24, 48, and 72 hours at 37 °C with 5% CO2. Following each interval, 300 µL of the initial eluate and 300 µL of the medium were used to dilute each eluate in a 1:1 ratio, resulting in a second eluate of 5 mg/mL.The plate was incubated for 24 hours after 100 µL of each eluate was added in quintuplicate [43]. Following the incubation period, 10 µL of MTT reagent (5 mg mL−1) dissolved in PBS was added to DMEM low glucose without phenol red, and the plates were rinsed twice with sterile PBS solution. Because MTT is photosensitive, the plates were shielded from light. 50 µL of sodium dodecyl sulfate (SDS) detergent solution was added after 4 hours of incubation at 37 °C with 5% CO2 to generate blue formazan crystals. Measurements were made using a UV-vis at a wavelength of 570 nm after 15 minutes of agitation. Equation 3 was used to compute cytotoxicity, with the untreated cells serving as the control group [44-46].

$$\% \text{ cellular visibility} = \frac{\text{tested absorbance}}{\text{control group}} \text{x } 100 \qquad \text{Eq. 3}$$

The control group was taken into consideration with 100% viability in order to calculate the proportion of viable cells. The International Organization Standard (ISO 10993-5), as described by Xiao [1] was used to classify cellular cytotoxicity. Grades 0 and 1 indicate non-cytotoxicity, while grades 2, 3, 4, and 5 indicate varying degrees of cytotoxicity, as indicated in **Table 3.**

Table 3. Levels of Cytotoxicity

level	Cellular activity
0	≥100%

1	≤99%
2	≤75%
3	≤49%
4	≤25%
5	= 0

The composites' cytotoxicity was evaluated indirectly using MC3T3-E1 cell line pre-osteoblasts and cultivated L929 cell line fibroblasts. An eluate with a concentration of 5 mg/mL was used for the test. Figures 3 A, B show the cell viability data. The medium that had been in touch with the composites for 24, 48, and 72 hours was applied to L929 fibroblast cells for 24 hours. The MTT colorimetric technique was used to assess the composites' cytotoxicity. For 24, 48, and 72 hours, MC3T3 pre-osteoblastic cells were exposed to the medium in contact with the composites. The MTT colorimetric technique was used to assess the composites' cytotoxicity. None of the composites were harmful to cell lines, as Figure 1 illustrates. According to the International Organization for Standardization (ISO) 10993-5[48], the findings are displayed in Table 2 and demonstrate more than 87% cytocompatibility of the composites with cells, displaying degree 1 or 0 of cytotoxicity.

Table 4. Levels of cytotoxicity of the composites

Levels of cytotoxicity

	Identification	**24 hrs**	**48 hrs**	**72 hrs**
L929	**NS-1**	1	1	1
	NS-1a	0	0	1
	NS-1b	0	0	0
	NS-1c	1	0	0
MC3T3	**NS-1**	1	0	1
	NS-1a	1	1	1
	NS-1b	1	1	1
	NS-1c	1	1	1

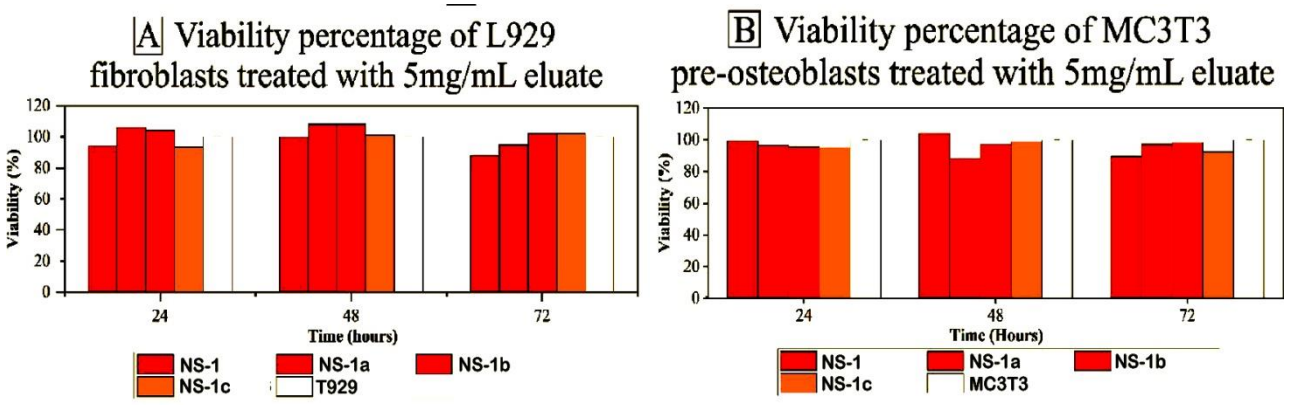

Figure 1. (A) Viability percentage of L929 fibroblasts treated with 5 mg/mL eluates containing composites HA-gelatin in different concentrations of PEG, at different experiment times, incubated for 24 hrs;

(B) viability percentage of MC3T3 pre osteoblasts treated with 5 mg/mL eluates containing composites HA-gelatin in different concentrations of PGG, at different experiment times, incubated for 24 hrs.

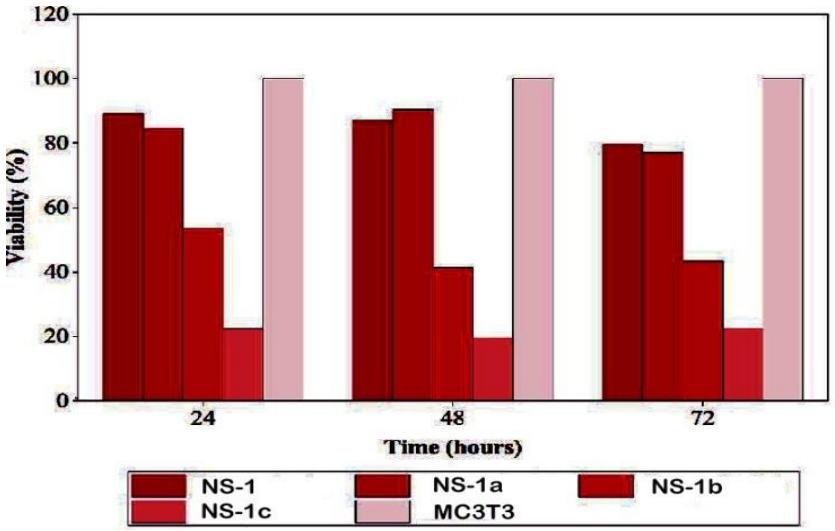

Figure 2. Viability percentage of MC3T3 pre osteoblasts treated with 10 mg/mL eluates containing composites HA-gelatin in different concentrations of PEG, at different times, incubated for 4 days.

The positive results were as expected as the materials used to manufacture the bionano-composites have already proven to be biocompatible. Furthermore, one of the main reasons why degrees 0 and 1 of cytotoxicity were obtained in both L929 fibroblasts and MC3T3 pre osteoblasts is due to the controlled release of composites.

3. Result and Discussion

Gelatin-coated poly-(ethyleneglycol)-hydroxyapatite [Gelatin-(HAp-PEG)] bio-nano-composites are synthesized for biomedical applications are characterized for enhanced biocompatibility, tunable mechanical properties, and, when an antimicrobial agent is added, significant antimicrobial effects. The synthesis typically involves a multistep process combining different techniques, HAp nanoparticles are commonly prepared first, often using a wet chemical precipitation which allows for control over particle size and morphology. The HAp nanoparticles are then integrated into a matrix involving PEG and gelatin.

Layer solvent casting, freeze drying, and lamination, as well as simple blending and photocrosslinking, are typically used to accomplish this. PEG is sometimes used as a template or a capping agent during HAp synthesis to control crystal growth and size. To improve stability and mechanical properties, the gelatin component is often cross-linked, for instance, using glutaraldehyde. Field emission-scanning electron microscopy (FE-SEM) is used to confirm the nanorod or spherical shape and uniform distribution of HAp particles within the polymer matrix. Fourier transform infrared spectroscopy (FTIR) is used to confirm the presence of characteristic functional groups of HAp, PEG,

and gelatin, and to identify chemical interactions or bonding between components.X-ray diffraction (XRD) analysis helps determine the crystalline nature of the HAp and the overall phase composition of the nanocomposite. HAP-PEG nanocomposites typically demonstrate low or negligible cytotoxicity (high biocompatibility) towards normal cells, especially osteoblast and fibroblast cell lines. The incorporation of Polyethylene Glycol (PEG) is specifically aimed at improving the biocompatibility and biodegradability of hydroxyapatite (HAp). In certain instances, HAP-PEG or analogous nanocomposites are investigated as drug carriers to augment the cytotoxic effects of anticancer medications specifically against cancer cells (for example, human gastric cancer cells) by facilitating sustained release and targeted delivery. In these applications, the objective is to increase the toxicity of the drug to cancer cells, while ensuring that the carrier remains predominantly non-toxic to the surrounding healthy tissues.

4. Conclusion

The novel HAp nanoparticle, HAp-PEG nanocomposite, and Gelatin-(HAp-PEG) bionanocomposite that were made and successfully prepared in this study were used to improve the crystallinity and antibacterial behavior of biomedical applications. The nanoparticle was made by an ionic gelation method using the PEG covalent bond cross-linking with HAp confirmed by FTIR. Amorphous HAp particles improved its crystallinity by PEG, revealed by X-ray diffraction pattern and SEM images exhibited the agglomeration of nanocomposite particles reduced gelatin to develop the exact hexagonal structure with good interfacial bonding and mechanical interlocking by the polymer matrix. Gelatin-(HAp-PEG) bio-nanocomposite, which has been interacting with and inactivating the essential enzymes of bacteria to lose its ability to replicate, resulting in cell death and significant bactericidal activity against E. coli (-ve) bacteria, may be a promising antibacterial agent. This composite is therefore a good candidate for bone fixation device. Therefore, they can be utilized to safeguard coffee beans, bamboo straws, and mandarins from these pathogens, enhancing their value and quality of use. The inherent characteristic of Gel-(HAP-PEG) bio-nano-composites is typically their absence of cytotoxicity, rendering them exceptionally suitable and promising options for a range of biomedical applications, including bone tissue engineering and drug delivery systems.

5. Acknowledgements

The authors are thankful to SAIF, CDRI, Lucknow and Dr H.S. Gour University Sagar (India), for providing spectral and analytical data of the Synthetic products. We are also grateful to Head, Department Chemistry, Govt. Science College Jabalpur M.P. for giving the facilities to carry out the works.

Reference

1. Mondal S, Dorozhkin SV, Pal U., Recent progress on fabrication and drug delivery applications of nanostructured hydroxyapatite. WIREs Nanomed. Nanobiotechnol. 2018;10:e1504.
2. Li, T.T.; Zhang, Y.; Ren, H.T., Peng, H.K.; Lou, C.W.; Lin, J.H. Two-step strategy for constructing hierarchical pore structured chitosan–hydroxyapatite composite scaffolds for bone tissue engineering. Carbohydr. Polym. 2021, 260, 117765.
3. Collins MN, Ren G, Young K, Pina S, Reis RL, Oliveira JM. Scaffold fabrication technologies and structure/function properties in bone tissue engineering. Adv Funct Mater 2021;31:2010609.
4. R. Parhi, "Cross-linked hydrogel for pharmaceutical applications: a review," Advanced Pharmaceutical Bulletin, vol. 7, no. 4, pp. 515–530, 2017.
5. S. M. F. Kabir, P. P. Sikdar, B. Haque, M. A. R. Bhuiyan, A. Ali, and M. N. Islam, "Cellulose-based hydrogel materials: chemistry, properties and their prospective applications," Progress in Biomaterials, vol. 7, no. 3, pp. 153–174, 2018.
6. Iglesias-Mejuto, A.; García-González, C.A. 3D-Printed, Dual Crosslinked and Sterile Aerogel Scaffolds for Bone Tissue Engineering. Polymers 2022, 14, 1211..
7. Jurak M, Wiącek AE, Ładniak A, Przykaza K, Szafran K. What affects the biocompatibility of polymers? Adv Colloid Interface Sci 2021;294:102451.
8. Civantos A, Martínez-Campos E, Ramos V, Elvira C, Gallardo A, Abarrategi A. Titanium coatings and surface modifications: toward clinically useful bioactive implants. ACS Biomater Sci Eng 2017;3:1245–61.
9. Koons GL, Diba M, Mikos AG. Materials design for bone-tissue engineering. Nat Rev Mater 2020;5:584–603.
10. Salim, S.A.; Loutfy, S.A.; El-Fakharany, E.M.; Taha, T.H.; Hussien, Y.; Kamoun, E.A. Influence of chitosan and hydroxyapatite incorporation on properties of electrospun PVA/HA nanofibrous mats for bone tissue regeneration: Nanofibers optimization and in-vitro assessment. J. Drug Deliv. Sci. Technol. 2021, 62, 102417.
11. Fu, L.; Wang, Z.; Dong, S.; Cai, Y.; Ni, Y.; Zhang, T.; Wang, L.; Zhou, Y. Bilayer poly(Lactic-co-glycolic acid)/nano- hydroxyapatite membrane with barrier function and Osteogenesis promotion for guided bone regeneration. Materials 2017, 10, 257.
12. Peng S, Jin G, Li L, Li K, Srinivasan M, Ramakrishna S, et al. Multi-functional electrospun nanofibres for advances in tissue regeneration, energy conversion & storage, and water treatment. Chem Soc Rev 2016;45:1225–41.
13. Xing, F.; Chi, Z.; Yang, R.; Xu, D.; Cui, J.; Huang, Y.; Zhou, C.; Liu, C. Chitin-hydroxyapatite-collagen composite scaffolds for bone regeneration. Int. J. Biol. Macromol. 2021, 184, 170–180
14. Wei Y, Chen M, Li M, Wang D, Cai K, Luo Z, et al. Aptamer/hydroxyapatite- functionalized titanium substrate promotes implant osseointegration via recruiting mesenchymal stem cells. ACS Appl Mater Interfaces 2022;14: 42915–30.
15. Chen F-M, Liu X. Advancing biomaterials of human origin for tissue engineering. Prog Polym Sci 2016;53:86–168.
16. Jain P, Kathuria H, Dubey N. Advances in 3D bioprinting of tissues/organs for regenerative medicine and in-vitro models. Biomaterials. 2022;287:121639.

17. Li H, Zhu YJ. Nanowires: Synthesis and energy/environmental applications. Energy Environ Mater 2021;4:544–61.
18. Kohli, N.; Sharma, V.; Orera, A.; Sawadkar, P.; Owji, N.; Frost, O.G.; Bailey, R.J.; Snow, M.; Knowles, J.C.; Blunn, G.W.; et al. Pro-angiogenic and osteogenic composite scaffolds of fibrin, alginate and calcium phosphate for bone tissue engineering. J. Tissue Eng. 2021, 12, 20417314211005610
19. Cai Y, Chang SY, Gan SW, Ma S, Lu WF, Yen C-C. Nanocomposite bioinks for 3D bioprinting. Acta Biomater 2022;151:45–69.
20. Mondal S, Nguyen TP, Pham VH, Hoang G, Manivasagan P, Kim MH, et al. Hydroxyapatite nano bioceramics optimized 3D printed poly lactic acid scaffold for bone tissue engineering application. Ceram Int 2020;46:3443–55.
21. Deng J, Song Q, Liu S, Pei W, Wang P, Zheng L, et al. Advanced applications of cellulose-based composites in fighting bone diseases. Compos Part B Eng. 2022: 110221.
22. Ileana Ielo, Giovanna Calabrese, Giovanna De Luca, Sabrina Conoci, Recent Advances in Hydroxyapatite-Based Biocomposites for Bone Tissue Regeneration in Orthopedics, Int. J. Mol. Sci., 2022, 23(17), 9721; https://doi.org/10.3390/ijms23179721
23. Indah Wahda, Syahruddin Kasim, Maming, Hasnah Natsir, St. Fauziah, Yusafir Hala, Andi Muhammad Anshar, Andriani Usman, Windasari, Indah Raya, Communications in Science and Technology, 2024, 9(1) 16–24.
24. Kim, H. W.; Knowles, J. C.; Kim, H. E. Porous scaffolds of gelatin-hydroxyapatite nanocomposites obtained by biomimetic approach: Characterization and antibiotic drug release. J. Biomed. Mater. Res., Part B 2005, 74 (2), 686−698.
25. GHANBARI, M.; SALAVATI-NIASARI, M.; MOHANDES, F. Nanocomposite scaffolds based on gelatin and alginate reinforced by Zn2SiO4 with enhanced mechanical and chemical properties for tissue engineering. Arabian Journal of Chemistry 2022, 15 (4), No. 103730.
26. Malik, M. H.; et al. Thyroxine-loaded chitosan/carboxymethyl cellulose/hydroxyapatite hydrogels enhance angiogenesis in in-ovo experiments. Int. J. Biol. Macromol. 2020, 145, 1162−1170.
27. CUI, N.; et al. Hyaluronic acid hydrogel scaffolds with a triple degradation behavior for bone tissue engineering. Carbohydr. Polym. 2015, 126, 192−198.
28. Malik, M. H.; et al. Thyroxine-loaded chitosan/carboxymethyl cellulose/hydroxyapatite hydrogels enhance angiogenesis in in-ovo experiments. Int. J. Biol. Macromol. 2020, 145, 1162−1170.
29. Dhandapani P., Siddarth Arun S., Kamalasekaran S., Maruthamuthu S., Rajagopal G., Polym. 2014, 103,448–455.
30. P. Boomi, H.G. Prabhu, P. Manisankar, S. Ravikumar, Study on antibacterial activity of chemically synthesized PANI-Ag-Au nanocomposite, Appl. Surf. Sci. 300 (2014) 66–72.
31. Mathew Peter, Nitya Ganesh, N. Selvamurugan, H. Tamura, R. Jayakumar, et al., Preparation and characterization of chitosan–gelatin/nanohydroxyapatite compos- ite scaffolds for tissue engineering applications, Carbohydr. Polym. 80 (2010) 687–694.
32. Marija Vukomanovic, Ines Bracko, Ida Poljansek, Dragan Uskokovic, Danilo Suvorov, et al., The growth of silver nanoparticles and their combination with hydroxyapatite to form composites via a sonochemical approach, Cryst. Growth Des. 11 (2011) 3802–3812.

33. Akhilesh K. Gaharwar, Sandhya A. Dammu, Jamie M. Canter, Wu. Chia-Jung, Gudrun Schmidt, Highly extensible, tough, and elastomeric nanocomposite hydrogels from poly(ethylene glycol) and hydroxyapatite nanoparticles, Biomacromolecules 12 (2011) 1641–1650.
34. Vojislav Stanic, Djordje Janackovi'c, Sladjana B. Tanaskovi'c, Dragoljub Jovanovi'c, Slavica Raicevi', et al., Synthesis of antimicrobial monophase silver-doped hydroxy- apatite nanopowders for bone tissue engineering, Appl. Surf. Sci. 257 (2011) 4510–4518.
35. S. Agnihotri, S. Mukherji, S. Mukherji, Size-controlled silver nanoparticles synthe- sized over the range 5–100 nm using the same protocol and their antibacterial effi- cacy, RSC Adv. 4 (2014) 3974–3983.
36. R.M. Tripathi, A. Saxena, N. Gupta, H. Kapoor, R.P. Singh, High antibacterial activity of silver nanoballs against E. coli MTCC 1302, S. typhimurium MTCC 1254, B. subtilis MTCC 1133 and P. aeruginosa MTCC 2295, Digest J. Nanomater. Biostruct. 5 (2010) **323–330.**
37. OROOJI, Y.; GHANBARI, M.; AMIRI, O.; SALAVATI- NIASARI, M. Facile fabrication of silver iodide/graphitic carbon nitride nanocomposites by notable photo-catalytic performance through sunlight and antimicrobial activity. J. Hazard Mater. 2020, 389, No. 122079.
38. ISO International Organization for Standardization Biological evaluation of medical devices - Part 5: Tests for in vitro cytotoxicity; ISO 10993−5; Geneva, Switzerland, 2009.
39. XIAO, S.; et al. Environment-friendly synthesis of trace element Zn, Sr, and F co-doping hydroxyapatite with non-cytotoxicity and improved osteoblast proliferation and differentiation. Biological Trace Element Research 2018, 185, 148−161.
40. HINZ, B.; et al. The myofibroblast: one function, multiple origins. American Journal of Pathology 2007, 170 (6), 1807−1816.
41. Pottathara, Y. B.; et al. Morphological, mechanical, and in-vitrobioactivity of gelatine/collagen/hydroxyapatite based scaffolds pre- pared by unidirectional freeze-casting. Polym. Test. 2021, 102, No. 107308.
42. Chen, P.; et al. Biomimetic composite scaffold of hydroxyapatite/ gelatin-chitosan core-shell nanofibers for bone tissue engineering. Mater. Sci. Eng., C 2019, 97, 325−335.
SATHIYAVIMAL, S.; et al. Biosynthesis and characterization of hydroxyapatite and its composite (hydroxyapatite-gelatin-chitosan- fibrin-bone ash) for bone tissue engineering applications. Int. J. Biol. Macromol. 2019, 129, 844−852.
43. BEGAM, H.; et al. MG63 osteoblast cell response on Zn-doped hydroxyapatite (HAp) with various surface features. Ceram. Int. 2017,
43 (4), 3752−3760.
44. Huang, L. H.; Han, J.; Ouyang, J. M.; Gui, B. S. Shape-dependent adhesion and endocytosis of hydroxyapatite nanoparticles on A7R5 aortic smooth muscle cells. J. Cell. Physiol. 2019, 235 (1), 465−479.
45. JUNG, G.-Y.; PARK, Y.-J.; HAN, J.-S. Effects of HA-released calcium ion on osteoblast differentiation. J. Mater. Sci.: Mater. Med.2010, 21, 1649−1654.
46. LIAO, H.; et al. Injectable calcium phosphate cement with PLGA, gelatin, and PTMC microspheres in a rabbit femoral defect. Acta Biomaterialia 2011, 7 (4), 1752−1759.